International Journal of Pharmaceutics 561 (2019) 74–81

Contents lists available at ScienceDirect

International Journal of Pharmaceutics

journal homepage: www.elsevier.com/locate/ijpharm

Cascade therapy with doxorubicin and survivin-targeted tailored nanoparticles: An effective alternative for sensitization of cancer cells to chemotherapy

Cenk Daglioglu[a,*], Fatma Necmiye Kaci[b]

[a] Izmir Institute of Technology, Faculty of Science, Department of Molecular Biology and Genetics, Urla/Izmir 35430, Turkey
[b] Erzurum Technical University, Faculty of Science, Department of Molecular Biology and Genetics, Yakutiye/Erzurum 25050, Turkey

ARTICLE INFO

Keywords:
Nanoparticles
Chemoresistance
Doxorubicin
Survivin
Colon cancer
Pancreatic cancer
Leukemia

ABSTRACT

Chemotherapy frequently involves combination treatment protocols to maximize tumor cell killing. Unfortunately these intensive chemotherapeutic regimes, often show disappointing results due to the development of drug resistance and higher nonspecific toxicity on normal tissues. In cancer treatment, it is critically important to minimize toxicity while preserving efficacy. We have previously addressed this issue and proposed a nanoparticle-based combination therapy involving both a molecularly targeted therapy and chemotherapeutic agent for neutralizing antiapoptotic survivin (*BIRC5*) to potentiate the efficacy of doxorubicin (DOX). Although the particles exhibited strong anticancer effect on the lung carcinoma A549 and the cervical carcinoma HeLa cells, there were lower-level therapeutic outcomes on the colon carcinoma HCT-116, the leukemia Jurkat and the pancreatic carcinoma MIA PaCa-2 cells. Since targeted therapies are one of the key approaches for overcoming drug resistance, tailoring the treatment of cancer cells with distinct characteristics is necessary to improve the therapeutic outcome of cancer therapy and to minimize potential pharmacokinetic interactions of drugs. In the light of this issue, this study examined whether a cascade therapy with low-dose DOX and survivin-targeted tailored nanoparticles is more effective at sensitizing HCT-116, Jurkat and MIA PaCa-2 cancer cells to DOX-chemotherapy than simultaneous combination therapy. The results demonstrated that the sequential therapy with the protocol comprising addition of the nanoparticles after incubation of cells with DOX clearly advanced the therapeutic outcome of related cancer cells, whereas the reverse protocol resulted in a reduction or delay in apoptosis, emphasizing the critical importance of formulating synergistic drug combinations in cancer therapy.

1. Introduction

Conventional chemotherapy uses individual anticancer agents or combinations for the treatment of malignant tumors (Chabner and Roberts, 2005). However, tumor cells often present challenges to chemotherapeutic agents due to multiple mutations endowing high levels of chemoresistance, which is a major obstacle for successful treatment (Holohan et al., 2013). One of the prominent factors responsible for the survival of tumor cells is activation of the inhibitor of apoptosis proteins (IAPs)-dependent antiapoptotic program, which produces resistance to chemotherapeutic agents (Fulda and Vucic, 2012). Therefore, this family of proteins has gained growing interest as drug targets to eliminate drug resistance. Survivin, a structurally unique member of IAP family, is one of the most cancer-specific proteins identified to date due to its biological function in apoptosis inhibition, proliferation enhancement and promoting angiogenesis, three key criteria for cancer growth and progression (Ryan et al., 2009). Since overexpression of survivin plays an important role in the drug-resistant phenotype of human cancer cells, it has become an attractive target to re-sensitize cancer cells to chemotherapeutic agents and provides opportunities for the development of targeted cancer therapies (Pennati et al., 2008). AICAR (5-aminoimidazole-4-carboxamide-1-β-D-ribofuranoside) is a novel small-molecule inhibitor of the heat shock protein 90 (Hsp90) and can serve as a nonpeptidic antagonist of the survivin-Hsp90 complex. This is achieved by mimicking the chemical and conformational properties of the recently described peptidic antagonist shepherdin; thereby destabilizing survivin by inhibiting the chaperone function which interrupts functional protein production (Meli et al., 2006). This implies that AICAR could be of potential value for increasing the sensitivity of cancer cells to anticancer agents, and could be easily incorporated in

* Corresponding author.
E-mail address: cenkdaglioglu@iyte.edu.tr (C. Daglioglu).

https://doi.org/10.1016/j.ijpharm.2019.02.036
Received 20 November 2018; Received in revised form 14 February 2019; Accepted 18 February 2019
Available online 27 February 2019
0378-5173/

practice for the downregulation of survivin as a small-molecule inhibitor.

Although remarkable efforts have been made in recent years to show survivin as a potential biomarker and molecular target in cancer therapy (Duffy et al., 2007; Altieri, 2008), recent studies attribute a role to survivin in normal physiology, especially in those cells undergoing self-renewal and proliferation (Fukuda and Pelus, 2006; Li and Brattain, 2006). Therefore, a long time exposure to anti-survivin therapy could affect the viability of these stem cells and tissue regeneration. In this context, targeted delivery is necessary for the translation of survivin therapy to the clinic in order to overcome issues of potential toxicity and broad side effects (Shapira et al., 2011). On the other hand, therapeutic agents with low molecular weight are rapidly cleared from the body and often suffer from a short half-life in blood (Markman et al., 2013). Therefore, another crucial factor ensuring the effectiveness of therapeutics is their bioavailability at the target site, which can be significantly improved via bioconjugation with a stable delivery system as we have reported previously (Daglioglu, 2017), thereby rendering improved pharmacokinetic performance at specific target sites.

Considering the potential importance of neutralizing survivin for enhancing tumor cell response to anticancer agents, we have previously developed a core/shell type vectorized nanoparticle formulation for simultaneous delivery of AICAR and DOX, and demonstrated its enhanced anticancer capability in five different tumor-derived cell lines (A549, HCT-116, HeLa, Jurkat and MIA PaCa-2) (Daglioglu and Okutucu, 2016; Daglioglu and Okutucu, 2017). Among all cancer cells tested, the nanoparticles show stronger anticancer effect on A549 and HeLa cells, whilst moderately inhibiting the growth of HCT-116, Jurkat and MIA PaCa-2 cells, most probably due to pharmacokinetic limitations of inhibitor/drug combination (Miao et al., 2017). Since this simultaneous combination treatment was found to be less effective in eliminating the large portion of chemoresistance on HCT-116, Jurkat and MIA PaCa-2 cells; in the present study, the effect of sequential combination therapy with low-dose DOX and survivin-targeted tailored nanoparticles was investigated as an alternative treatment protocol to determine the most successful synergistic route in cancer therapy. For this purpose, an improved AICAR delivery platform [Fe_3O_4@SiO_2(FITC)-BTN/FA/AICAR] with tailored dual-targeting feature was synthesized to enhance nanoparticle accumulation by simultaneously targeting multiple receptors on cancer cells, according to the method previously described (Daglioglu, 2018). In an effort to provide an extended and safer synergistic inhibition method to increase susceptibility of cancer cells to chemotherapy, cancer cells were sequentially exposed to IC_{50} dose of Fe_3O_4@SiO_2(FITC)-BTN/FA/AICAR nanoparticles (50 μg/mL) and a low concentration of DOX (20 nM), which is 5 times lower than the mean plasma concentration of DOX in patients under chemotherapy (Minotti et al., 2004), with the following protocols: (1) DOX alone; (2) the nanoparticles alone; (3) addition of the nanoparticles after incubation of cells with DOX; (4) addition of DOX after incubation of cells with the nanoparticles. The cell tests demonstrated that exposure to the nanoparticles after incubation of cells with DOX significantly increased anticancer activity of DOX when compared with cells exposed to reverse protocol, and caused an increased rate of apoptosis compared to simultaneous combination protocol. This confirmed that when designing inhibitor/drug combinations, tailoring the interaction of inhibitors and drugs is of crucial importance to achieve more effective combination therapy in the treatment of a broad range of cancers.

2. Material and methods

2.1. Materials

Propidium iodide (PI), RNase A, 3-(4,5-dimethylthiazol-2-yl)-2,5-diphenyltetrazolium bromide (MTT), trypsin, proteinase inhibitor cocktail, bovine serum albumin (BSA), acrylamide, bisacrylamide, TRIS base, sodium dedocyl sulfate (SDS), ammonium persulfate (APS), tetramethylethylenediamine (Temed), glycine, Tween-20, non-fat milk powder, methanol (CH_3OH) and phosphate buffered saline tablet (PBST) were purchased from *Sigma-Aldrich Chemicals*. DMEM growth medium, RPMI-1640 growth medium, 10% Fetal bovine serum (FBS), streptomycin, penicillin and L-glutamic acid were purchased from *Gibco Life technologies*. BCA protein assay kit, horseradish peroxidase (HRP) substrate and PVDF membrane were purchased from *Thermo Fisher Scientific*. 7-aminoactinomycin (7-AAD) and PE-annexin-V were purchased from *BD Biosciences*. Caspase-3 colorimetric assay kit was purchased from *BioVision, Inc (USA)*. Anti-mouse survivin antibody, anti-mouse β-actin antibody and anti anti-mouse HRP-conjugated seconder antibody were purchased from *Cell Signaling Technology (CST)*. All other chemicals and reagents were of the highest purity. All the experiments were performed in deionized Milli-Q water.

2.2. Cell cultures

HCT-116 (human epithelial colorectal carcinoma), Jurkat (human acute T-cell leukemia) and MIA PaCa-2 (human epithelial pancreatic carcinoma) cell lines were kindly provided by Biotechnology and Bioengineering Research and Application Centre, Izmir Institute of Technology, Turkey. HCT-116 and MIA PaCa-2 cancer cells were cultured in Dulbecco's modified Eagle medium (DMEM) supplemented with 10% fetal bovine serum (FBS), 100 μg/ml streptomycin, 100 U/ml penicillin and 2 mM L-glutamic acid; Jurkat cancer cells were cultured in Roswell Park Memorial Institute-1640 (RPMI-1640) growth medium supplemented with 10% fetal bovine serum (FBS), 100 μg/ml streptomycin, 100 U/ml penicillin and 2 mM L-glutamic acid. All cell lines were incubated in 5% CO_2 and 90–100% relative humidity at 37 °C. Medium renewal was carried out 2–3 times per week, and cells were subcultured when they achieved 80–90% confluence.

2.3. Synthesis and characterization of nanoparticles

The silica magnetic-fluorescence based biotin (BTN) and folic acid (FA) functionalized Fe_3O_4@SiO_2(FITC)-BTN/FA/AICAR nanoparticle platform was synthesized to deliver antitumoral inhibitor AICAR into cancer cells as described in our previous work (Daglioglu, 2018). Briefly, Fe_3O_4 nanocrystals were synthesized by a simple co-precipitation of Fe^{+2}/Fe^{+3} salts which were then encapsulated within a SiO_2 shell to provide surface modification and biocompatibility as well as to act as a host for fluorescent dye (FITC) via microemulsion sol–gel chemistry. To ensure quick and efficient cellular internalization of the nanoparticles in tumor cells, the Fe_3O_4@SiO_2(FITC) structure was co-vectorized with BTN and FA moieties via an esterification reaction for exploitation overexpressed vitamin receptors on cancer cells with dual-targeting concept. Lastly, AICAR was successfully attached on the amine-modified nanoparticles via pH-labile schiff-base formation which endowed pH-switched inhibitor release property to the nanoparticles. The efficiency of AICAR conjugation and physicochemical properties of the nanoparticles were characterized based on the combination of several techniques as described (Daglioglu and Okutucu, 2016; Daglioglu, 2018).

2.4. Cellular uptake analysis

Internalization of the nanoparticles and the presence of DOX inside the cell were visualized using an Olympus IX71 fluorescence microscope equipped with an appropriate filter set. Images were acquired using a CCD camera and analyzed using ImageJ advanced version software. HCT-116, Jurkat and MIA PaCa-2 cells (1×10^5 cells/well) were seeded in 6-well plates overnight before experiments, and then sequentially exposed to Fe_3O_4@SiO_2(FITC)-BTN/FA/AICAR nanoparticles (50 μg/mL) and a low-dose DOX (20 nM) for 6 h, at intervals of 3 h, in 5% CO_2 at 37 °C. Microscopic images in the green channel for

detection of the FITC label encapsulated in nanoparticles, in the red channel for detection of DOX, in the blue channel for detection of DAPI and in the bright-field were obtained by fluorescence microscopy.

2.5. Cell viability analysis

The cytotoxic effects of the sequential combination protocols with Fe_3O_4@SiO_2(FITC)-BTN/FA/AICAR nanoparticles and a low-dose DOX were evaluated using MTT cell proliferation assay. HCT-116, Jurkat and MIA PaCa-2 cells were seeded into 96-well plates at a density of 1×10^4 per well in 100 μL of media and grown overnight. The cells were then incubated with different sequential treatment protocols with DOX (20 nM) and the nanoparticles (50 μg/mL) either alone or in sequential combination: DOX alone for 48 h; the nanoparticles alone for 48 h; DOX alone for 24 h and then the nanoparticles for another 24 h; the nanoparticles alone for 24 h and then DOX for another 24 h, at 37 °C under 5% CO_2. Following this incubation, cells were incubated in medium containing 0.5 mg/mL of MTT for 4 h. The medium was discarded, and the precipitated formazan violet crystals were dissolved in 150 μL of DMSO to solubilize the formazan. After shaking the plate for 10 min, the absorbance of the sample was measured at 570 nm by a multi-detection microplate reader. The absorbance of dissolved formazan in the visible region correlates with the number of intact active cells. The percentage of viable cells was calculated according to the following equation:

$$\text{Cell viability}(\%) = (M_{\text{nanoparticles/free drugs}} - M_{\text{blank}})/(M_{\text{control}} - M_{\text{blank}}) \times 100$$

where $M_{\text{nanoparticles/free drugs}}$ is the absorbance of the cells, growth medium and nanoparticles or free drugs, M_{control} is the absorbance of the cell and growth medium, and M_{blank} is the absorbance of the growth medium alone.

2.6. Detection of apoptotic cells by flow cytometry

The percentage of cells undergoing apoptosis induced by the sequential combination protocols was measured using flow cytometry with 7-AAD and PE-annexin-V staining. HCT-116, Jurkat and MIA PaCa-2 cells (1×10^5 cells/well) were seeded in 6-well plates with 2 mL of medium overnight before experiments. The cells were then incubated with different treatment protocols with low-dose DOX (20 nM) and the nanoparticles (50 μg/mL) either alone or in sequential combination: DOX alone for 6 h; the nanoparticles alone for 6 h; DOX alone for 3 h and then the nanoparticles for another 3 h; the nanoparticles alone for 3 h and then DOX for another 3 h, at 37 °C under 5% CO_2. Before analysis, the cells were carefully washed with cold PBS, digested with trypsin (except Jurkat) and collected by centrifugation. The cells were washed twice with cold PBS, resuspended in 200 μL of annexin binding buffer and stained with 10 μL of 7-AAD and PE-annexin-V. The stained cells were first incubated for 15 min at room temperature in the dark, and then analyzed by flow cytometry. The untreated cells incubated with medium alone were used as the controls. Unstained cells, cells stained with PE-annexin-V alone and cells stained with 7-AAD alone were used to set up compensation and quadrants. Flow cytometric analysis was performed on a FACS (Facscanto; Becton Dickinson, San Jose, CA) by counting 10,000 events.

2.7. Caspase-3 catalytic activity assay

Changes in caspase-3 enzyme activity of the cells are an important sign of apoptosis. To assess the effect of the sequential combination protocols on cell death, caspase-3 activity was analyzed fluorometrically by means of the Caspase-3/CPP32 colorimetric assay kit according to the manufacturer's instructions (BioVision Inc, USA). The cancer cells (5×10^5 cells/well) were treated with low-dose DOX (20 nM) and the nanoparticles (50 μg/mL), as follows: DOX alone for 48 h; the nanoparticles alone for 48 h; DOX alone for 24 h and then the nanoparticles for another 24 h; the nanoparticles alone for 24 h and then DOX for another 24 h, at 37 °C under 5% CO_2. This method is based on the hydrolysis of the peptide substrate N-acetyl-Asp-Glu-Val-Asp-p-nitroanilide (DEVD-pNA) by caspase-3, resulting in the release of the p-nitroaniline moiety. p-Nitroaniline was measured at 405 nm using plate reader.

2.8. Western blot analysis

The downregulation of survivin induced by the sequential combination protocols was determined by western blotting. HCT-116, Jurkat and MIA PaCa-2 cells were seeded in 75 cm^2 flasks at a density of 5×10^6 cells and grown overnight. The cells were then treated with low-dose DOX (20 nM) and the nanoparticles (50 μg/mL), as follows: DOX alone for 48 h; the nanoparticles alone for 48 h; DOX alone for 24 h and then the nanoparticles for another 24 h; the nanoparticles alone for 24 h and then DOX for another 24 h, at 37 °C under 5% CO_2. After this incubation, the cells were homogenized in lysis buffer supplemented with proteinase inhibitor cocktail for 30 min on ice, and the supernatant was collected after centrifugation at 12,000 rpm. Protein content was determined using the BCA protein assay kit. Lysates (20 μg) were separated using 5–15% sodium dodecyl sulfate polyacrylamide gel electrophoresis and transferred onto PVDF membranes. Membranes were blocked in 5% non-fat milk in PBST (PBS with 0.05% Tween-20) buffer for 1 h at room temperature. After blocking, the membrane was incubated overnight at 4 °C in PBST buffer containing a mouse primary antibody to survivin (1:2000). The membrane was then washed three times with PBST buffer and incubated with secondary antibody (anti anti-mouse HRP-conjugated seconder antibody) with a 1:10000 dilution for 2 h. Survivin protein was detected using HRP substrate solution by chemiluminescence system according to the manufacturer's instructions (PerkinElmer, Waltham, MA). β-Actin protein expression served as an internal control.

2.9. Cell cycle analysis by flow cytometry

To determine the antiproliferative effects of the sequential combination protocols against HCT-116, Jurkat and MIA PaCa-2 cells, cell cycle distributions were analyzed by flow cytometry-based propidium iodide (PI) staining. The cells (2×10^5 cells/well) were seeded in 6-well plates with 2 mL of medium overnight before experiments and then incubated with different sequential treatment protocols with low-dose DOX (20 nM) and the nanoparticles (50 μg/mL), as follows: DOX alone for 24 h; the nanoparticles alone for 24 h; DOX alone for 12 h and then the nanoparticles for another 12 h; the nanoparticles alone for 12 h and then DOX for another 12 h, at 37 °C under 5% CO_2. After the incubation, the cells were trypsinized, washed once with PBS and fixed in 80% ethanol overnight at −20 °C. The next day, after centrifugation of fixed cells, the pellet washed with cold PBS and then resuspended in DNA staining solution [200 μL 0.1% Triton X-100 in PBS, 20 μL (200 μg/mL) RNase A and 20 μL (1 mg/mL) propidium iodide] for 30 min at room temperature. The stained cells were analyzed using flow cytometer.

2.10. Statistical analysis

All data were represented as means ± standard deviation (SD). Statistical analysis was performed with the Student's *t* test by comparing two groups. A P value of ≤ 0.05 was considered statistically significant.

3. Results and discussion

3.1. Synthesis and characterization of nanoparticles

The Fe_3O_4@SiO_2(FITC)-BTN/FA/AICAR nanoparticles consisted of

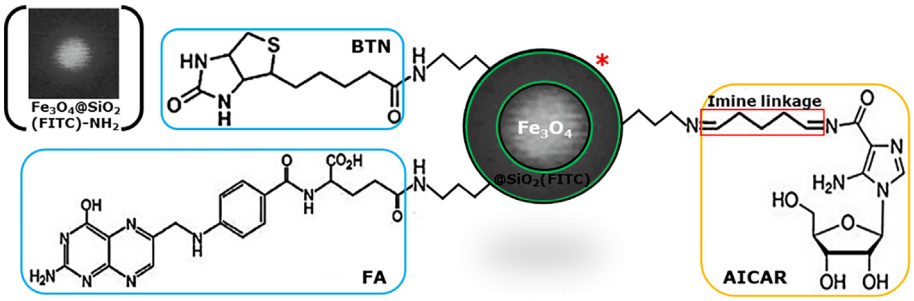

Fig. 1. Schematic representation of Fe_3O_4@SiO_2(FITC)-BTN/FA/AICAR nanoparticles. *The core-shell structure of the nanoparticle (white core-gray shell) was obtained from the scanning transmission electron microscopy (STEM). (For interpretation of the references to color in this figure legend, the reader is referred to the web version of this article.)

silica-coated luminomagnetic nanomaterials (serving as both a magnetic and an optical contrast agent), triple conjugated to BTN, FA and AICAR as described Daglioglu and Okutucu (2016); Daglioglu (2018). To increase the cellular uptake and accumulation, the outermost layer of nanoparticles was functionalized with BTN and FA molecules by means of an esterification reaction. The silica surface was then conjugated with AICAR by pH-labile imine linkage for environmentally responsive drug release, with the expectation that this acid-sensitive linkage would promote AICAR release into the more acidic endosome of cancer cells instead of in the systemic circulation environment. The quantitative study of AICAR conjugation on the silica surface showed that 6.1 μM of AICAR were conjugated per mg Fe_3O_4@SiO_2(FITC)-BTN/FA/AICAR nanoparticles. The average hydrodynamic diameter of the nanoparticle formulation was about 50 nm with narrow size distribution (Fig. 1).

3.2. Cellular uptake

The cellular uptake of Fe_3O_4@SiO_2(FITC)-BTN/FA/AICAR nanoparticle vector and low-dose DOX by HCT-116, Jurkat and MIA PaCa-2 cells was studied by fluorescence microscopy. DAPI was used as a nuclear counterstain to follow the intracellular internalization. As seen in Fig. 2, the spatial localization of the nanoparticles was confirmed by the appearance of green fluorescence in all cells, which clearly indicated the successful penetration of the vectors into the cells in 3 h. The overlap of green FITC fluorescence and red DOX fluorescence was observed from the merged images of the nanoparticles and free DOX at 6 h (total 3 h DOX and 6 h NPs incubation, and vice versa), confirming the endocytotic uptake of both the nanoparticles and DOX in the cancer cells. After additional 3 h incubation periods of both the nanoparticles and DOX to 6 h, the fluorescence intensity of the nanoparticles and DOX were increased due to the greater accumulation of the compounds. It should be noted that no significant difference in the cellular uptake of the nanoparticles was observed between the cancer cells, which was consistent with our previous findings of the ability of dual-targeting function that simultaneously target multiple receptors on cancer cells resulting in a strong cellular uptake of nanoparticles (Daglioglu, 2018). Importantly, enhanced cellular uptake of nanoparticles would undoubtedly facilitate the sensitization effect of AICAR and thereby improving the therapeutic efficacy of DOX.

3.3. Cell viability analysis

To examine how the sequential combination therapy of Fe_3O_4@SiO_2(FITC)-BTN/FA/AICAR nanoparticles with a low-dose DOX affected the cytotoxic activity, the proliferations of HCT-116, Jurkat, and MIA PaCa-2 cells treated with different protocols were evaluated using MTT cell proliferation assay. Since the cancer cells had similar IC_{50} values (~50 μg/mL: the concentration required for 50% cell death) after 48 h exposure the nanoparticle formulations ranging from 0.1 to 200 μg/mL (Daglioglu and Okutucu, 2016), in this study all subsequent experiments were carried out at 50 μg/mL concentration of the nanoparticles in sequential combination with low-dose DOX (20 nM). It was found that the sequential therapy with the protocol comprising addition of DOX prior to the incubation of nanoparticles significantly inhibited cancer cell growths as compared to cells exposed to each drug alone and reverse protocol (Fig. 3). This protocol showed high cytotoxicity to all the cells tested, whereas the reverse protocol attenuated DOX-mediated cytotoxicity in HCT-116 cells, demonstrating that the potentiation effect of AICAR on DOX-mediated cytotoxicity in the colon carcinoma is subject to sequence-dependent treatment. This synergy also occurred almost with the same levels in Jurkat cells. Moreover, MIA PaCa-2 cells responded to both protocols but gave better result with the first protocol and increased the efficacy of chemotherapy. A siRNA/DOX based sequence-dependent combination therapy has also been reported in breast and pancreatic adenocarcinomas (Ghosh et al., 2014). This demonstrated prominent sequence dependence in neutralizing the actions of survivin with the same course as seen in HCT-116 and Jurkat cells. In contrast, another siRNA/DOX based study reported that exposure to DOX after incubation of cells with survivin siRNA significantly inhibited cell growth in several drug-resistant lung cancer cells (Yonesaka et al., 2006). These observations suggest that DOX induced cytotoxicity in the drug-sensitive cancer cells, but it also caused upregulation of survivin, reducing its cytotoxic effect. The subsequent depletion of survivin resulted in efficient cell death, which may also prevent cells from becoming resistant. On the other hand, pretreatment with a survivin inhibitor before DOX chemotherapy might promote cell death by increasing sensitivity to anticancer drugs especially in drug-resistant cancer cells and could lead to an obvious resistance reversing, confirming the vital importance of tumor-type-dependent cancer therapy.

3.4. Detection of apoptotic cells by flow cytometry

The impact of the sequential combination therapy on proapoptotic activity against HCT-116, Jurkat, and MIA PaCa-2 cells was investigated by analyzing the proportion of apoptotic cells by flow cytometry with 7-AAD/PE-annexin-V double staining. The treatment protocol comprising addition of the nanoparticles after incubation of cells with DOX, versus the other treatments, strongly increased the percent of double positive (PEannexin-V^+/7-AAD^+) apoptotic cells in HCT-116, Jurkat, and MIA PaCa-2 cells to 92.8 / 90.0 and 67.1%, respectively, which are improved percentages compared to simultaneous combination treatment (60.5/59.4 and 45.0%, respectively) as previously described Daglioglu and Okutucu (2017). The treatment with reverse protocol lowered the number of late apoptotic cells in HCT-116 (82.5%), Jurkat (72.4%) and MIA PaCa-2 (55.4%) cells, demonstrating that the reverse protocol led to prolonged initial phase of apoptosis and resulted in a delay or reduction in apoptosis (Fig. 4). These results suggested that exposing the cancer cells to the low-dose DOX after incubation of nanoparticles caused upregulation of survivin, and its inhibitory effect on apoptosis correlates with expression levels of survivin in different tumor types. Based on these observations, it has been previously reported that the combination of a survivin mutant gene with DOX was not more effective than each drug alone in enhancing apoptosis in breast and colorectal adenocarcinomas (Mesri et al., 2001), suggesting that the synergistic potential of therapeutics against

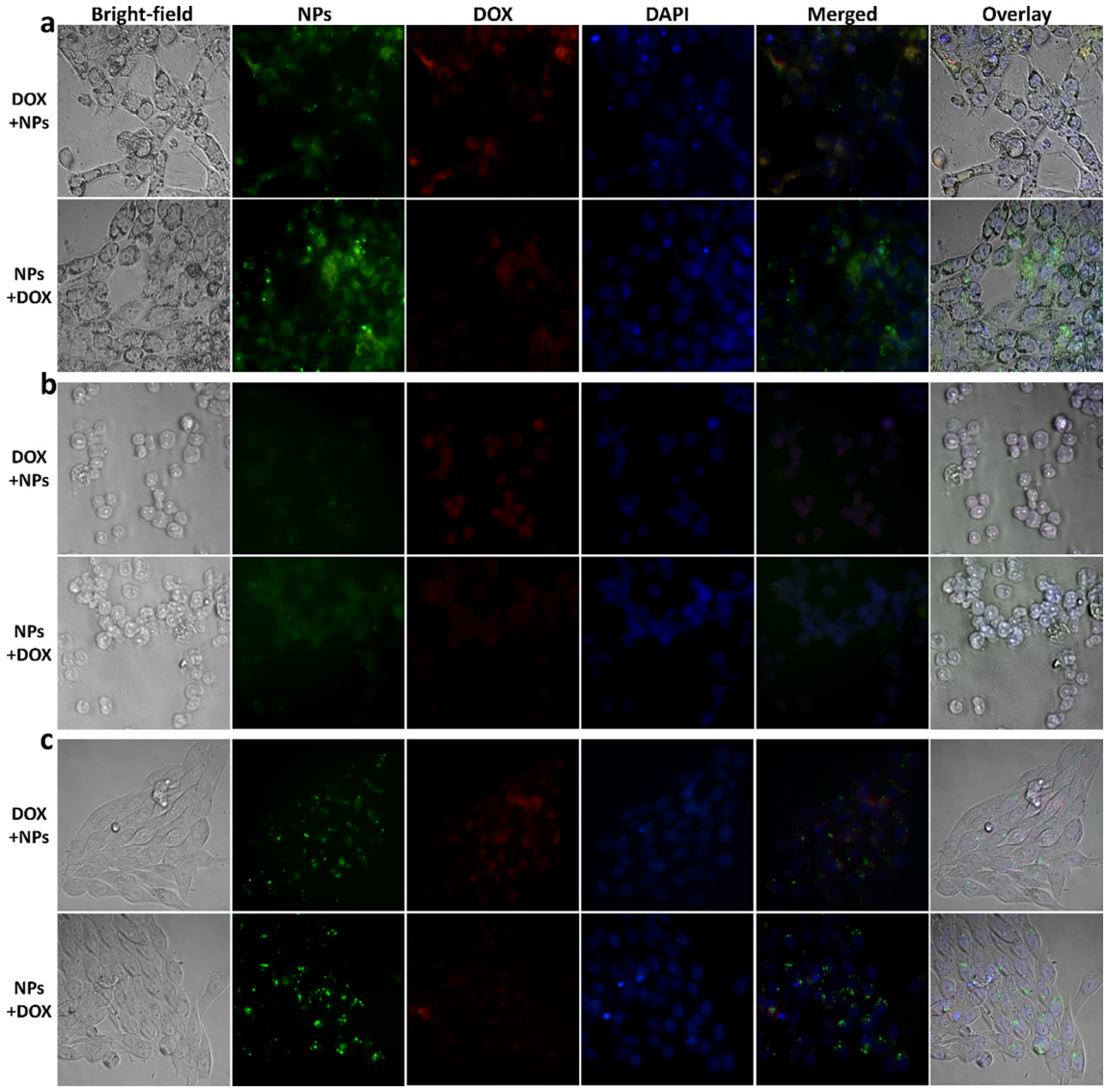

Fig. 2. Fluorescence microscopy images of (a) HCT-116, (b) Jurkat and (c) MIA PaCa-2 cells after incubation with Fe_3O_4@SiO_2(FITC)-BTN/FA/AICAR nanoparticles and free DOX for 3 and 6 h (DOX alone for 3 h and then the NPs for another 3 h; the NPs alone for 3 h and then DOX for another 3 h). The nanoparticles were observed as green fluorescence, DOX was observed as red fluorescence and DAPI was observed as blue fluorescence. For columns: 1, bright-field images; 2, fluorescence images of NPs; 3, fluorescence images of DOX; 4, the stained nuclei of cells with DAPI; 5, the merger of NPs, DOX and DAPI; and 6, overlay of bright-field images and fluorescence images. (For interpretation of the references to colour in this figure legend, the reader is referred to the web version of this article.)

apoptosis may exhibit a cell-type-dependent manner related to biochemical profiles of cancer cells or drug pharmacokinetics.

3.5. Caspase-3 activity assay

To additionally test the apoptotic effects of the treatment protocols on HCT-116, Jurkat and MIA PaCa-2 cells, the cells were evaluated by measuring caspase-3 activity, since survivin binds to caspase-3 and inhibit its activation (Tamm et al., 1998). Consistent with the analysis of apoptosis by flow cytometry, an increased caspase-3 activity was observed in the all cells exposed to DOX for 24 h followed by the nanoparticles treatment for another 24 h, whereas the reverse protocol induced less caspase-3 enzyme activity, explaining the reason of prolonged initial stage of apoptosis in flow cytometry results (Fig. 5). On the other hand, when compared with the simultaneous combination treatment, the caspase-3 activity was increased from approximately 170% to 220% in HCT-116 cells, but no significant differences were obtained in Jurkat and MIA PaCa-2 cells (Daglioglu and Okutucu, 2017). As expected, these results also revealed that the sequence of administration (drug application) is important for sensitizing cancer cells to chemotherapy and the course is strictly depends on the character of each cell type.

3.6. Western blotting

To determine the survivin downregulation effects of the sequential combination treatments on HCT-116, Jurkat and MIA PaCa-2 cells, the cell lysates were analyzed for survivin by western blot. The sequential therapy with the protocol comprising addition of DOX prior the incubation of nanoparticles exhibited reduced expression of survivin at high level on HCT-116 and Jurkat cells, and moderate level on MIA PaCa-2 cells, whereas the reverse protocol attenuated the effect of nanoparticles and caused upregulation of survivin in all the cancer cells tested. Moreover, the nanoparticles treatment successfully inhibited expression of survivin as compared to low-dose DOX treatment (Fig. 6). These results corroborated that low-dose DOX plays an important role in inducing the expression of survivin and thus lowering the effect of nanoparticles against cancer cells as seen in the reverse protocol

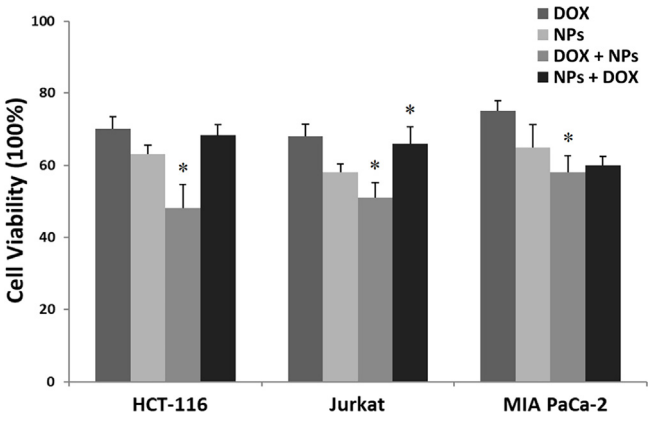

Fig. 3. Cell viability of HCT-116, Jurkat and MIA PaCa-2 cells treated with DOX alone for 48 h; Fe_3O_4@SiO_2(FITC)-BTN/FA/AICAR nanoparticles alone for 48 h; DOX alone for 24 h and then the nanoparticles for another 24 h; the nanoparticles alone for 24 h and then DOX for another 24 h. The results are expressed as percentage of cell viability or cell number obtained in the untreated controls. Each column represents the mean ± SD of three independent experiments performed in triplicate normalized to non-treated cells (taken as 100%), $*p < 0.05$ in comparison with DOX or NPs.

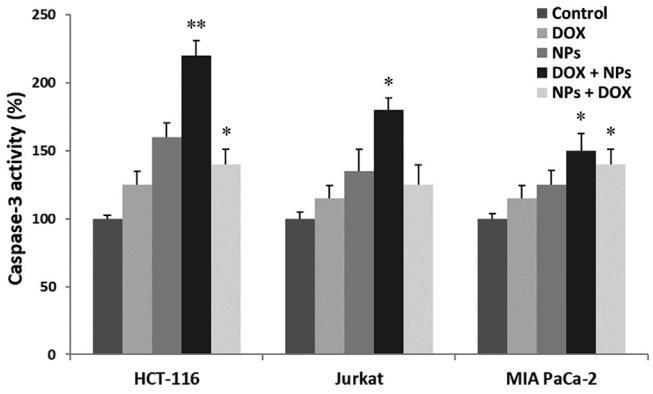

Fig. 5. Effects of the sequential combination therapies on caspase-3 activation of HCT-116, Jurkat and MIA PaCa-2 cells. Caspase-3 activity was measured in cell lysates treated with DOX alone for 48 h; Fe_3O_4@SiO_2(FITC)-BTN/FA/AICAR nanoparticles alone for 48 h; DOX alone for 24 h and then the nanoparticles for another 24 h; the nanoparticles alone for 24 h and then DOX for another 24 h. Caspase-3 activity was analyzed fluorometrically by means of hydrolysis of fluorogenic substrate N-acetyl-Asp-Glu-Val-Asp-pNA (DEVD-pNA). Each column represents the mean values (± SD) of three independent experiments normalized to non-treated cells (taken as 100%), $**p < 0.01$ and $*p < 0.05$ as compared to no treatment.

experiments, which is in line with the previous studies that have demonstrated that an anti-survivin agent potentiates the anticancer activity of low-dose DOX in a sequence dependent manner (Ghosh et al., 2014).

3.7. Cell cycle analysis by flow cytometry

To further investigate whether the sequential combination protocols would promote the antiproliferation of cancer cells, analysis of cell

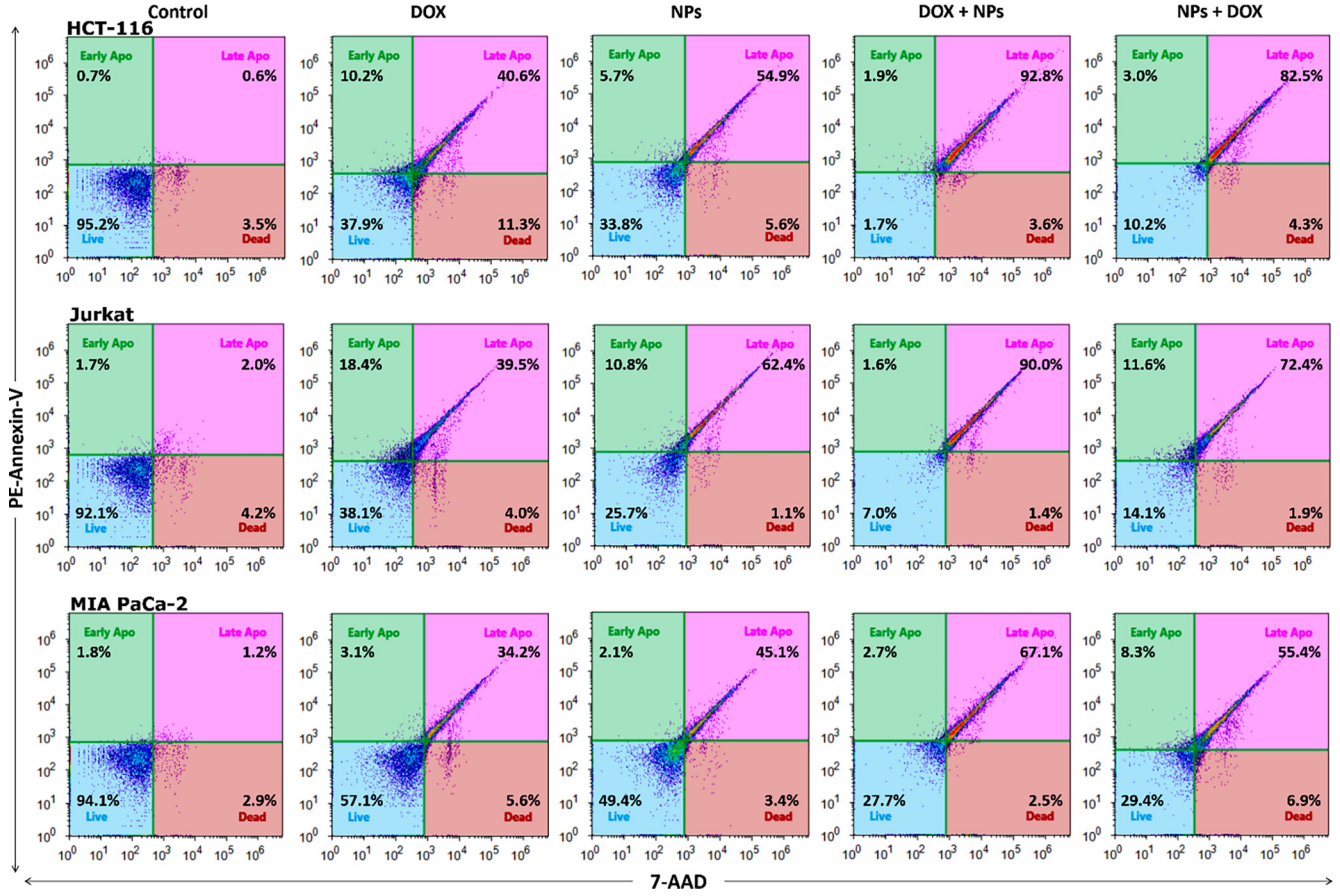

Fig. 4. Apoptosis analysis of HCT-116, Jurkat and MIA PaCa-2 cells treated with DOX alone for 6 h; Fe_3O_4@SiO_2(FITC)-BTN/FA/AICAR nanoparticles alone for 6 h; DOX alone for 3 h and then the nanoparticles for another 3 h; the nanoparticles alone for 3 h and then DOX for another 3 h, by flow cytometry. Viable cells labelled with PE-annexin-V(−)/7-AAD(−), early apoptotic cells labelled with PE-annexin-V(+)/7-AAD(−) and apoptotic cells labelled with PE-annexin-V(+)/7-AAD(+) in flow cytometric graphics. Non-treated cells were used as control.

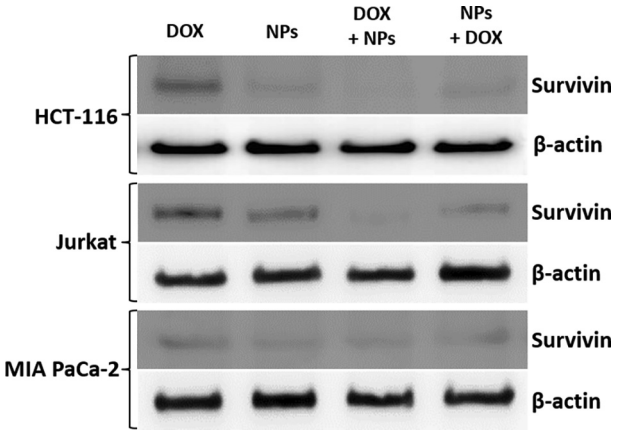

Fig. 6. Downregulation of Survivin after the sequential combination treatments. HCT-116, Jurkat and MIA PaCa-2 cells were exposed to DOX alone for 48 h; Fe_3O_4@SiO_2(FITC)-BTN/FA/AICAR nanoparticles alone for 48 h; DOX alone for 24 h and then the nanoparticles for another 24 h; the nanoparticles alone for 24 h and then DOX for another 24 h. The lysate proteins were analyzed for survivin and β-actin expression by western blotting. The expression of β-actin served as an internal control.

cycle phase distribution was performed using flow cytometry (Fig. 7). The sequential therapy with the protocol comprising addition of the nanoparticles after incubation of cells with DOX significantly increased the cell population at G_2/M phase (from 13.7 to 55.5% in HCT-116; from 14.7 to 81.0% in Jurkat; from 20.8 to 48.4% in MIA-PaCa2), whereas the reverse protocol exhibited lower portion of arrest in the G_2/M checkpoint (40.3% in HCT-116; 71.8% in Jurkat; 42.3% in MIA-PaCa2) due to the delayed progression in S phase, which is consistent with the result of apoptosis. However, both sequential therapies did not enhance cell cycle arrest in the cancer cells, compared to the simultaneous combination treatment in our previous work (Daglioglu and Okutucu, 2017). The simultaneous combination treatment arrested more cells at the G_2/M phase (60.0% in HCT-116; 96.1% in Jurkat; 70.5% in MIA-PaCa2) compared to both sequential therapy, could be attributed to the cellular uptake capacity of free DOX is lower than its conjugated form. The population of G_2/M phase (63.6% in HCT-116; 84.5% in Jurkat; 65.0% in MIA-PaCa2) induced by conjugated DOX treatment was more than 2-fold compared to the population of G_2/M phase (24.5% in HCT-116; 28.8% in Jurkat; 29.3% in MIA-PaCa2) induced by free DOX treatment. On the other hand, the cell cycle distribution of the cells exposed to the nanoparticles alone was found to be similar with the untreated cells. However the nanoparticle treatment shifted cells to the subG1 phase, a hallmark of late-stage apoptosis, and demonstrated that proliferating cells engaged in apoptosis. It has been previously reported that survivin binds and inhibits caspase-3, controlling the G_2/M checkpoint of the cell cycle by inhibiting apoptosis and promoting proliferation (Li et al., 1998; Li et al., 1999).

4. Conclusion

Herein the efficacy of sequential therapy format of survivin-targeted tailored Fe_3O_4@SiO_2(FITC)-BTN/FA/AICAR nanoparticles and low-dose DOX was investigated to determine the optimal combination cancer therapy for the colon carcinoma HCT-116, the leukemia Jurkat and the pancreatic carcinoma MIA PaCa-2 cells. These cascade therapies were examined by using flow cytometric analyses of apoptosis with 7-AAD/PE-annexin-V staining and cell cycle with propidium iodide DNA staining. In addition, caspase-3 activity and western blot assays were performed to reveal activation levels of caspase-3 and down-regulation of survivin, supporting the flow cytometric data. Furthermore, fluorescence microscopy and cytotoxicity studies confirmed intracellular accumulation of drugs and their antitumor activity. The results indicated that exposure to the nanoparticles after incubation of cells with DOX clearly advanced the therapeutic outcome of cancer cells and exhibited improved antitumor activity. The reverse protocol resulted in a reduction or delay in apoptosis due to the upregulation of

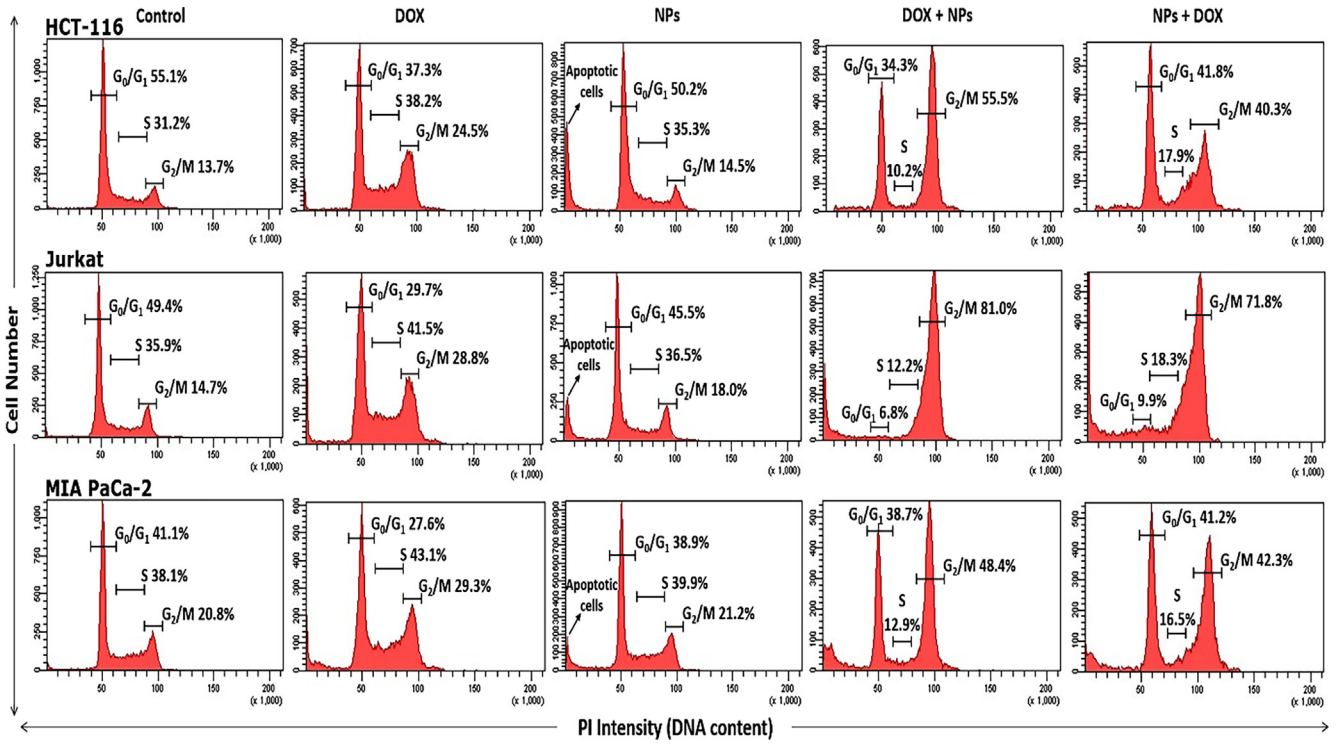

Fig. 7. Effect of the sequential combination therapies on the cell cycle distribution of HCT-116, Jurkat and MIA PaCa-2 cells treated with DOX alone for 24 h; Fe_3O_4@SiO_2(FITC)-BTN/FA/AICAR nanoparticles alone for 24 h; DOX alone for 12 h and then the nanoparticles for another 12 h; the nanoparticles alone for 12 h and then DOX for another 12 h, determined by flow cytometry-based PI staining. Non-treated cells were used as control. SubG1 shows the degree of late stage apoptosis.

survivin after low-dose DOX treatment, which led to inhibition of caspase-3, a crucial component of apoptotic cell death. On the other hand, the reverse protocol (pretreatment with nanoparticles before DOX chemotherapy) may be more effective against drug-resistant cancer cells and might promote sensitivity to DOX by reversing drug resistance with pre-inhibition of survivin (20). In conclusion, the present results demonstrate the importance of systemic administration of drug combinations, and have the potential for the identification of possible new uses of already known drugs in improving the therapeutic outcome of cancer therapy.

Acknowledgments

The authors would like to thank TUBITAK (The Scientific and Technological Research Council of Turkey) Incentive Program for International Scientific Publications for financial assistance (355155, 371332), Professor Alper Arslanoglu at the Izmir Institute of Technology for providing the opportunity to work in his laboratory, all members of Department of Molecular Biology and Genetics and High Technology Research and Application Center of Erzurum Technical University for their technical support, and Dr. Mark Thompson for proofreading the manuscript.

Declaration of interest

The authors report no declarations of interest.

References

Altieri, D.C., 2008. Survivin, cancer networks and pathway-directed drug discovery. Nat. Rev. Cancer 81, 61–70.
Chabner, B.A., Roberts Jr., T.G., 2005. Timeline: chemotherapy and the war on cancer. Nat. Rev. Cancer 5, 65–72.
Daglioglu, C., 2017. Enhancing tumor cell response to multidrug resistance with pH-sensitive quercetin and doxorubicin conjugated multifunctional nanoparticles. Colloids Surf. B Biointerfaces 156, 175–185.
Daglioglu, C., 2018. Environmentally responsive dual-targeting nanoparticles: improving drug accumulation in cancer cells as a way of preventing anticancer drug efflux. J. Pharm. Sci. 107, 934–941.
Daglioglu, C., Okutucu, B., 2016. Synthesis and characterization of AICAR and DOX conjugated multifunctional nanoparticles as a platform for synergistic inhibition of cancer cell growth. Bioconjug. Chem. 27, 1098–1111.
Daglioglu, C., Okutucu, B., 2017. Therapeutic effects of AICAR and DOX conjugated multifunctional nanoparticles in sensitization and elimination of cancer cells via survivin targeting. Pharm. Res. 34, 175–184.
Duffy, M.J., O'Donovan, N., Brennan, D.J., Gallagher, W.M., Ryan, B.M., 2007. Survivin: a promising tumor biomarker. Cancer Lett. 2491, 49–60.
Fukuda, S., Pelus, L.M., 2006. Survivin, a cancer target with an emerging role in normal adult tissues. Mol. Cancer Ther. 5, 1087–1098.
Fulda, S., Vucic, D., 2012. Targeting IAP proteins for therapeutic intervention in cancer. Nat. Rev. Drug Disc. 11, 109–124.
Ghosh, S.K., Yigit, M.V., Uchida, M., Ross, A.W., Barteneva, N., Moore, A., Medarova, Z., 2014. Sequence-dependent combination therapy with doxorubicin and a survivin-specific small interfering RNA nanodrug demonstrates efficacy in models of adenocarcinoma. Int. J. Cancer 134, 1758–1766.
Holohan, C., Van Schaeybroeck, S., Longley, D.B., Johnston, P.G., 2013. Cancer drug resistance: an evolving paradigm. Nat. Rev. Cancer 13, 714–726.
Li, F., Ambrosini, G., Chu, E.Y., Plescia, J., Tognin, S., Marchisio, P.C., Altieri, D.C., 1998. Control of apoptosis and mitotic spindle checkpoint by survivin. Nature 396, 580–584.
Li, F., Ackermann, E.J., Bennett, C.F., Rothermel, A.L., Plescia, J., Tognin, S., Villa, A., Marchisio, P.C., Altieri, D.C., 1999. Pleiotropic cell-division defects and apoptosis induced by interference with survivin function. Nat. Cell. Biol. 1, 461–466.
Li, F., Brattain, M.G., 2006. Role of the survivin gene in pathophysiology. Am. J. Pathol. 169, 1–11.
Markman, J.L., Rekechenetskiy, A., Holler, E., Ljubimova, J.Y., 2013. Nanomedicine therapeutic approaches to overcome cancer drug resistance. Adv. Drug Deliv. Rev. 65, 1866–1879.
Meli, M., Pennati, M., Curto, M., Daidone, M.G., Plescia, J., Toba, S., Altieri, D.C., Zaffaroni, N., Colombo, G., 2006. Small-molecule targeting of heat shock protein 90 chaperone function: rational identification of a new anticancer lead. J. Med. Chem. 49, 7721–7730.
Mesri, M., Wall, N.R., Li, J., Kim, R.W., Altieri, D.C., 2001. Cancer gene therapy using a suvivin mutant adenovirus. J. Clin. Inv. 108, 981–990.
Miao, L., Guo, S., Lin, C.M., Liu, Q., Huang, L., 2017. Nanoformulations for combination or cascade anticancer therapy. Adv. Drug Deliv. Rev. 115, 3–22.
Minotti, G., Menna, P., Salvatorelli, E., Cairo, G., Gianni, L., 2004. Anthracyclines: molecular advances and pharmacologic developments in antitumor activity and cardiotoxicity. Pharmacol. Rev. 56 (185), 229.
Pennati, M., Folini, M., Zaffaroni, N. Targeting, survivin in cancer therapy, 2008. Expert opin. Ther. Targets 124, 463–476.
Ryan, B.M., O'Donovan, N., Duffy, M.J., 2009. Survivin: a new target for anti-cancer therapy. Cancer Treat. Rev. 35, 553–562.
Shapira, A., Livney, Y.D., Broxterman, H.J., Assaraf, Y.G., 2011. Nanomedicine for targeted cancer therapy: towards the overcoming of drug resistance. Drug Resist. Updat. 14, 150–163.
Tamm, I., Wang, Y., Sausville, E., Scudiero, D.A., Vigna, N., Oltersdorf, T., Reed, J.C., 1998. IAP-family protein survivin inhibits caspase activity and apoptosis induced by Fas (CD95), Bax, caspases, and anticancer drugs. Cancer Res. 58, 5315–5320.
Yonesaka, K., Tamura, K., Kurata, T., Satoh, T., Ikeda, M., Fukuoka, M., Nakagawa, K., 2006. Small interfering RNA targeting survivin sensitizes lung cancer cell with mutant p53 to Adriamycin. Int. J. Cancer 118, 812–820.